blood

2011 117: 1986-1997
Prepublished online December 6, 2010;
doi:10.1182/blood-2010-05-284810

A small-molecule inhibitor of D-cyclin transactivation displays preclinical efficacy in myeloma and leukemia via phosphoinositide 3-kinase pathway

Xinliang Mao, Biyin Cao, Tabitha E. Wood, Rose Hurren, Jiefei Tong, Xiaoming Wang, Wenjie Wang, Jie Li, Yueping Jin, Wenxian Sun, Paul A. Spagnuolo, Neil MacLean, Michael F. Moran, Alessandro Datti, Jeffery Wrana, Robert A. Batey and Aaron D. Schimmer

Blood (print ISSN 0006-4971, online ISSN 1528-0020), is published weekly by the American Society of Hematology, 2021 L St, NW, Suite 900, Washington DC 20036.

A small-molecule inhibitor of D-cyclin transactivation displays preclinical efficacy in myeloma and leukemia via phosphoinositide 3-kinase pathway

Xinliang Mao,[1,2] Biyin Cao,[1] Tabitha E. Wood,[2,3] Rose Hurren,[2] Jiefei Tong,[4] Xiaoming Wang,[2] Wenjie Wang,[1] Jie Li,[1] Yueping Jin,[1] Wenxian Sun,[1] Paul A. Spagnuolo,[2] Neil MacLean,[2] Michael F. Moran,[4,5] Alessandro Datti,[6,7] Jeffery Wrana,[5,6] Robert A. Batey,[3,5] and Aaron D. Schimmer[2,5]

[1]Cyrus Tang Hematology Center, Jiangsu Institute of Hematology, First Affiliated Hospital, Soochow University, Suzhou, China; [2]Ontario Cancer Institute, Princess Margaret Hospital, Toronto, ON; [3]Department of Chemistry, The University of Toronto, Toronto, ON; [4]Program in Molecular Structure and Function, Hospital for Sick Children, University of Toronto, Toronto, ON; [5]McLaughlin Centre for Molecular Medicine, University of Toronto, Toronto, ON; [6]Samuel Lunenfeld Research Institute, Mount Sinai Hospital, Toronto, ON; and [7]Department of Experimental Medicine and Biochemical Sciences, University of Perugia, Perugia, Italy

D-cyclins are universally dysregulated in multiple myeloma and frequently overexpressed in leukemia. To better understand the role and impact of dysregulated D-cyclins in hematologic malignancies, we conducted a high-throughput screen for inhibitors of cyclin D2 transactivation and identified 8-ethoxy-2-(4-fluorophenyl)-3-nitro-2H-chromene (S14161), which inhibited the expression of cyclins D1, D2, and D3 and arrested cells at the G_0/G_1 phase. After D-cyclin suppression, S14161 induced apoptosis in myeloma and leukemia cell lines and primary patient samples preferentially over normal hematopoietic cells. In mouse models of leukemia, S14161 inhibited tumor growth without evidence of weight loss or gross organ toxicity. Mechanistically, S14161 inhibited the activity of phosphoinositide 3-kinase in intact cells and the activity of the phosphoinositide 3-kinases α, β, δ, and γ in a cell-free enzymatic assay. In contrast, it did not inhibit the enzymatic activities of other related kinases, including the mammalian target of rapamycin, the DNA-dependent protein kinase catalytic subunit, and phosphoinositide-dependent kinase-1. Thus, we identified a novel chemical compound that inhibits D-cyclin transactivation via the phosphoinositide 3-kinase/protein kinase B signaling pathway. Given its potent antileukemia and antimyeloma activity and minimal toxicity, S14161 could be developed as a novel agent for blood cancer therapy. (*Blood*. 2011;117(6):1986-1997)

Introduction

D-cyclins regulate cell-cycle progression and proliferation by acting in a complex with cyclin dependent kinases (CDKs) to promote the phosphorylation of the retinoblastoma protein and initiate cellular transition from G_1 to the S phase.[1] Overexpression of D-cyclins occurs in many tumors and leads to increased cell proliferation[2-4] and chemoresistance.[5] In contrast, inhibition of the expression of D-cyclins, either directly or indirectly, decreases cellular proliferation and induces apoptosis.[6-8]

In multiple myeloma, D-cyclins are universally dysregulated.[9] In primary patient samples, 54% overexpress cyclin D1, 48% overexpress cyclin D2, 3% overexpress cyclin D3, and 8% overexpress both cyclin D1 and cyclin D2.[9] Likewise, D-cyclins are overexpressed in a subset of patients with acute myeloid leukemia and are associated with poor outcome.[10] In myeloma, the overexpression of D-cyclins contributes to pathogenesis and chemoresistance.[2,4,9] For example, patients with increased cyclin D2 expression, especially in conjunction with other oncogenes such as c-maf, MafB, and FGFR3/MMSET, have an inferior event-free survival.[11]

Small molecules that inhibit D-cyclin transactivation can be useful probes to better understand the regulation of these proteins in leukemia and myeloma and can potentially be developed to cure such diseases. For example, glucocorticoids regulate D-cyclin expression by promoting the ubiquitination and proteasomal degradation of the oncogene c-maf by increasing the expression of the SP1 transcription factor that promotes ubiquitin expression.[12,13] The appetite-stimulant cyproheptadine decreases D-cyclin expression and induces cell death in myeloma cells through a mechanism distinct from the drug's known activity as an H1 histamine and serotonin receptor antagonist.[14] Finally, the natural product kinetin riboside inhibits transactivation of cyclins D1 and D2 by upregulating the expression of the transcription repressor isoforms of the cyclic adenosine monophosphate–responsive element modulator (CREM).[15] Some of these compounds, such as dexamethasone, are clinically used for myeloma treatment or are being tested in a clinical setting for refractory leukemia treatment.

Here, we conducted a chemical screening to identify inhibitors of the human cyclin D2 promoter using NIH3T3 cells engineered to overexpress the cyclin D2 promoter driving firefly luciferase.[12] From this screening, we identified the novel compound 8-ethoxy-2-(4-fluorophenyl)-3-nitro-2H-chromene (S14161), which inhibited D-cyclin transactivation via inhibition of phosphoinositide 3-kinase (PI3K) activity. Moreover, this compound displayed preclinical activity in myeloma and leukemia cells in vitro and in vivo.

Submitted May 12, 2010; accepted November 27, 2010. Prepublished online as Blood First Edition paper, December 6, 2010; DOI 10.1182/blood-2010-05-284810.

The online version of this article contains a data supplement.

The publication costs of this article were defrayed in part by page charge payment. Therefore, and solely to indicate this fact, this article is hereby marked "advertisement" in accordance with 18 USC section 1734.

Methods

Cell lines

All human myeloma cell lines were maintained in Iscove's modified Dulbecco medium (Gibco, Invitrogen). Human and murine leukemia cell lines were maintained in RPMI 1640 medium. All media were supplemented with 10% fetal bovine serum (FBS; HyClone), 100 μg/mL penicillin, and 100 U/mL streptomycin (HyClone).

High-throughput screening for inhibitors of cyclin D2 transactivation

A chemical screening for inhibitors of cyclin D2 transactivation was performed as described previously.[12] Briefly, NIH3T3 cells stably expressing c-maf and the cyclin D2 promoter driving firefly luciferase (3000 cells per well) were plated in 384-well plates by a Biomek FX liquid handler (Beckman Coulter). After the cells had adhered, they were treated with aliquots of the chemical compounds from the Maybridge Screening Collection of 56 000 organic compounds (Maybridge Chemical Company) at a final concentration of 5μM in 0.1% dimethyl sulfoxide (DMSO) at 37°C for 16 hours. After incubation, cyclin D2 transactivation was assessed by the luciferase assay.

Luciferase assay

Luciferase activity was assessed as described previously with Bright-Glo luciferase substrate (Promega).[12] The luminescence signal was detected with a 384-well Luminoskan luminescence plate reader (Thermo Labsystems) with a 5-second integration.

Cell growth and viability

Cell growth and viability were assessed with the MTS [3-(4,5-dimethylthiazol-2-yl)-5-(3-carboxymethoxyphenyl)-2-(4-sulfophenyl)-2H-tetrazolium] assay with a CellTiter96 AQ_{ueous} Non-Radioactive Assay kit (Promega) according to the manufacturer's instructions. Apoptosis was measured by flow cytometry to detect annexin V staining and propidium iodide uptake (Biovision) as described previously.[16]

Real-time reverse-transcription PCR

First-strand cDNA was synthesized from 1 μg of DNase-treated total cellular RNA with random primers and SuperScript II reverse transcriptase (Invitrogen) according to the manufacturer's instructions. Real-time reverse-transcription polymerase chain reaction (PCR) assays were performed in triplicate with 5 ng of RNA equivalent cDNA, SYBR Green PCR Master Mix (Applied Biosystems), and 400 nM gene-specific primers. Reactions were processed and analyzed on an ABI 7900 Sequence Detection System (Applied Biosystems). Forward/reverse PCR primer pairs for human cDNA were as follows: Cyclin D2, 5′-TGCAGAAGGACATCCAACC-3′/5′-AGGAACATGCAGACA-GCACC-3′; cyclin D3, 5′-AGTATGGAGCT-GCTGTGTTGC-3′/5′-AAGACTTCCTCC-TCACAG-CG-3′; and 18S, 5′-AGGAATTGACGGAAGGGCAC-3′/5′-GGACATCTAAG-GGCAT-CACA-3′. Relative mRNA expression was determined by the $^{\Delta\Delta}$CT method as described previously.[12]

Immunoblotting assay

Whole-cell lysates were prepared in RIPA lysis buffer from myeloma and leukemia cells as described previously.[12] Equal amounts of protein were subjected to sodium dodecyl sulfate–polyacrylamide gel electrophoresis followed by transfer to polyvinylidene difluoride membranes. Membranes were then probed with various antibodies. Anti–cyclin D1, anti–cyclin D3, anti–caspase-3, anti–poly(ADP ribose) polymerase, anti–protein kinase B (anti–AKT), anti–phospho-AKT (Ser473), anti–Mcl-1, anti–CDK9, anti–Bcl-2, and anti–Bad were purchased from Cell Signaling Technology Inc; anti–human cyclin D2 was purchased from Santa Cruz Biotechnology Inc; anti–Bim was purchased from Biovision; and anti–β-actin, anti–tubulin, and anti–GAPDH were purchased from Sigma-Aldrich. Secondary horseradish peroxidase–conjugated goat anti–mouse or anti–rabbit IgG was purchased from Amersham Bioscience UK. Detection was performed by the enhanced chemical luminescence method (Pierce).

Cell-cycle analysis

After treatment, cells were harvested, washed with cold phosphate-buffered saline (PBS), suspended in 70% cold ethanol, and incubated overnight at −20°C. Cells were washed and treated with 100 ng/mL DNase-free RNase (Invitrogen) at 37°C for 30 minutes, washed with cold PBS, and resuspended in PBS with 50 μg/mL propidium iodine. DNA content was analyzed by flow cytometry (FACSCalibur, Becton Dickinson). The percentage of cells in each phase of the cell cycle was calculated with ModiFit software (Becton Dickinson).

In vivo studies

Human leukemia cells (K562; 5×10^6) were injected subcutaneously into SCID mice. When tumors were palpable, tumors were excised and single-cell suspensions prepared. Cells (0.5×10^6) were reinjected subcutaneously into SCID mice. In a separate model, another human leukemia cell line (U937; 4×10^6) was injected subcutaneously into sublethally irradiated NOD-SCID mice. In both xenograft models, when tumors were palpable, mice were treated with S14161 (100 mg/kg body weight) in PBS containing 10% Tween 80 and 10% DMSO or vehicle control daily for 10 days. Tumor volume (tumor length × width^2 × 0.5236) was measured over time with calipers.[14] Mouse body weight was also monitored over time. For protein detection from xenografts after S14161 treatment, tumors were first excised and snap-frozen in liquid nitrogen. All samples were stored at −80°C for further study as reported previously.[14]

Cyclin D2 transfection with nanoparticle vectors

To improve DNA transfection efficiency in leukemia cells, we used ImagenFect RNAi (IR) nanoparticles (Nanomics Biopharm Inc). For 6-well plates, K562 cells were seated at 2 million per 2 mL per well in fresh medium 2 hours before transfection. To prepare the nano-IR-DNA complexes, 8 μg of pcDNA3.1-CCND2 plasmids or empty vectors (pcDNA3.1; Invitrogen) was diluted into 250 μL of complete medium that contained 10% fetal calf serum, and at the same time, 10 μL of IR nanovectors was diluted in 250 μL of complete medium and incubated for 10 minutes at room temperature. Next, the diluted nanoparticles were mixed well with diluted DNA and incubated for 20 minutes at room temperature. When they were ready, the complexes were added dropwise to cells and incubated in a 37°C incubator for 4 hours, followed by the addition of 1.5 mL of fresh medium and continuation of culturing for another 18 hours. Cells were then separated into aliquots for cyclin D2 expression analysis or were treated further with S14161 for 24 hours and used for apoptosis analysis.

AKT phosphorylation analysis

Various leukemia and myeloma cell lines were maintained overnight in Iscove's modified Dulbecco medium that contained 0.5% fetal calf serum, followed by treatment with 100 mM S14161 or LY294002 or DMSO. Cells were then stimulated with 100 ng/mL human recombinant insulin-like growth factor-1 (IGF1; PeproTech) for 10 minutes before being lysed in RIPA buffer that contained 1 mM orthovanadate. After clarification, cell lysates were subjected to Western blotting analysis with anti–phospho-AKT(Ser473) or anti-AKT.

Kinase activity in cell-free assay

The effects of S14161 on PI3K-associated enzyme activity were determined with HotSpot technology (Reaction Biology Corp). Briefly, recombinant PI3Ks, AKTs, phosphoinositide-dependent kinase-1 (PDK1), and mammalian target of rapamycin (mTOR; prepared from baculovirus in Sf21 insect cells by Millipore) and substrates were diluted in reaction buffer (20 mM HEPES [*N*-2-hydroxyethylpiperazine-*N*′-2-ethanesulfonic acid], pH 7.5, 10 mM $MgCl_2$, 1 mM EGTA [ethyleneglycotetraacetic acid], 0.02% Brij-35,

0.02 mg/mL bovine serum albumin, 1 mM Na_3VO_4, 2 mM dithiothreitol, 1% DMSO). After dilution, 5 nL of serial diluted S14161 was added with the Echo 550 liquid handler (Labcyte Inc). The reaction was started by adding hot adenosine triphosphate into the reaction mixture (final concentration was 10μM) and was stopped after 2 hours of incubation at room temperature. Free hot adenosine triphosphate was washed away before detection.

Immunoprecipitation of PI3K and PI3K activity evaluation by ELISA

To evaluate the effects of S14161 on PI3Ks derived from blood cancer cells, leukemia K562 and myeloma LP1 cells were lysed in ice-cold Buffer A (20 mM Tris [tris(hydroxymethyl)aminomethane]-HCl, pH 7.4, 137 mM NaCl, 1 mM CaCl2, 1 mM $MgCl_2$, and 0.1 mM sodium orthovanadate) plus 1% NP-40 and 1 mM phenylmethanesulfonyl fluoride, followed by clarification with high-speed centrifugation. Supernatants (200 μg of protein) were incubated with anti-p85 antibody (Millipore) overnight at 4°C followed by incubation with 60 μL of a 50% slurry of protein A agarose beads (Beyotime Institute of Biotechnology) with gentle rotation at 4°C for 2 hours. Purified PI3Ks were incubated for 2 hours at 37°C with 10μM substrate $PI(4,5)P_2$; 0, 3, 10, 30, 100, or 300μM S14161; or 10μM LY294002 in KBZ reaction buffer (Echelon Biosciences Inc). The product was then analyzed with PI3K activity enzyme-linked immunosorbent assay (ELISA) kits (Echelon Biosciences) according to the manufacturer's instructions.

To evaluate the inhibition of S14161 on PI3K in vivo, myeloma cells (OPM2) were maintained overnight in Iscove's modified Dulbecco medium that contained 0.5% fetal calf serum. Cells were then treated with DMSO, 100μM S14161, or LY294002 for 2 hours, followed by 100 ng of IGF1 for 10 minutes. Cells were harvested and washed in ice-cold Buffer A. Afterward, cells were lysed in Buffer A plus 1% NP-40 and 1 mM phenylmethanesulfonyl fluoride for 20 minutes. After clarification at high speed at 4°C, cell lysates were incubated with anti-p85 antibody (Millipore) overnight at 4°C, followed by incubation with 60 μL of a 50% slurry of protein A agarose beads with gentle rotation at 4°C for 2 hours. Purified PI3Ks were then incubated for 2 hours at 37°C with 10μM substrate $PI(4,5)P_2$. The product $PI(3,4,5)P_3$ was analyzed with PI3K activity ELISA kits.

Immunofluorescence assay

OPM2 myeloma cells were maintained in 0.5% serum overnight, followed by incubation with S14161 (100μM, 1 hour), LY294002 (100μM, 30 minutes), or DMSO (1 hour). Cells were then stimulated with 100 ng/mL IGF1 for 10 minutes and harvested in Tris-buffered saline that contained 1 mM sodium orthovanadate. Fifty thousand cells were transferred to coated slides (Fisher Scientific) with a Cytospin centrifuge. After they were air-dried for 20 minutes at room temperature, cells were fixed in 2% paraformaldehyde and permeabilized in 0.1% Triton X-100 for 5 minutes. After they were blocked in Tris-buffered saline with 5% bovine serum albumin for 30 minutes, cells were stained with AKT or phospho-AKT (1:150) overnight at 4°C in a humidifying container. Cells were then washed and incubated with rhodamine red–conjugated goat anti–rabbit IgG (1:100 vol/vol; Invitrogen). The subcellular location and relative abundance of AKT and phospho-AKT were analyzed with an Olympus FluoView 1000 laser scanning confocal microscope (Olympus America Inc).

Results

Identification of small-molecule inhibitors of D-cyclins by high-throughput screening

To better understand the regulation of D-cyclins and the effects of targeting their expression in myeloma and leukemia cells, we conducted a chemical screening for inhibitors of the human cyclin D2 promoter using NIH3T3 cells engineered to overexpress the cyclin D2 promoter-driven firefly luciferase (Promega). From a screening of the 56 000 compounds from the Maybridge Chemical Collection, we identified 531 compounds that reduced luciferase expression $> 50\%$ when tested at a final concentration of 5μM. These compounds were evaluated in secondary screenings, after which we identified 11 compounds, the most active of which was S14161 (Figure 1A), which reproducibly inhibited transactivation of the cyclin D2 promoter but did not inhibit transactivation of an unrelated Rous sarcoma virus promoter driving luciferase (Figure 1B) and did not reduce growth and viability of NIH3T3 in an MTS assay (data not shown).

Given the identification of S14161 as a potential inhibitor of cyclin D2 transactivation, we evaluated its effects on D-cyclin expression in myeloma and leukemia cell lines. Myeloma and leukemia cell lines were treated with S14161 for 24 hours followed by D-cyclin protein measurement with an immunoblotting assay. D-cyclin expression varied among cell lines, but at least 1 of the 3 D-cyclins (D1, D2, and D3) in the examined cell lines was decreased by S14161 (Figure 1C), and the inhibition of S14161 on cyclin D expression was concentration dependent, as shown in Figure 1D. These cell lines were subject to a range of events[9] that dysregulated D-cyclins, including cyclin D1 translocation (KMS12), c-maf overexpression (RPMI-8226, KMS11, LP1, JJN3), and FGFR3 translocation (KMS11), which indicated that S14161 might down-regulate D-cyclins via a specific pathway that controls or bypasses those events.

S14161 regulates D-cyclin expression on the transcriptional level rather than the translational or posttranslational levels

S14161 repressed cyclin D2 promoter-driven but not Rous sarcoma virus promoter–driven luciferase expression (Figure 1B). S14161 inhibited luciferase expression in a concentration-dependent manner (data not shown), and this inhibition was confirmed by cyclin D2 and cyclin D3 mRNA. As analyzed by quantitative real-time PCR, mRNA expression of both D2 and D3 was decreased by S14161 (Figure 1F), consistent with our identification of S14161 through a screening for inhibitors of D-cyclin transactivation (Figure 1B). To further evaluate the effects of S14161 on D-cyclin on the translational or posttranslational levels, we made a construct of cyclin D2 under the control of a cytomegalovirus promoter in the pcDNA3.1 vector (Invitrogen) and then analyzed the cyclin D2 decrease by S14161. S14161 at 5 or 10μM markedly decreased endogenous cyclin D expression in KMS11 and K562, as shown in Figure 1D; however, at the same concentration, S14161 displayed minimal effects on cyclin D2 expression, which was controlled by the cytomegalovirus promoter (Figure 1E). These results demonstrated that S14161 down-regulated cyclin D expression on the transcriptional but not translational level.

CDK9 is a portion of the elongation factor pTEFb (positive transcription elongation factor b) and performs a complementary function by phosphorylating Ser-2 in the carboxy-terminal domain of RNA polymerase II, which is required for transcript elongation.[17,18] To examine whether cyclin D was decreased by S14161 via the CDK9 signaling pathway, we checked expression of CDK9 in the myeloma cell lines LP1 and OPM2. CDK9 was decreased by S14161 in both LP1 and OPM2 cells within 24 hours in a concentration-dependent manner (Figure 1H), which further demonstrated that S14161 regulates cyclin D on the transcriptional level.

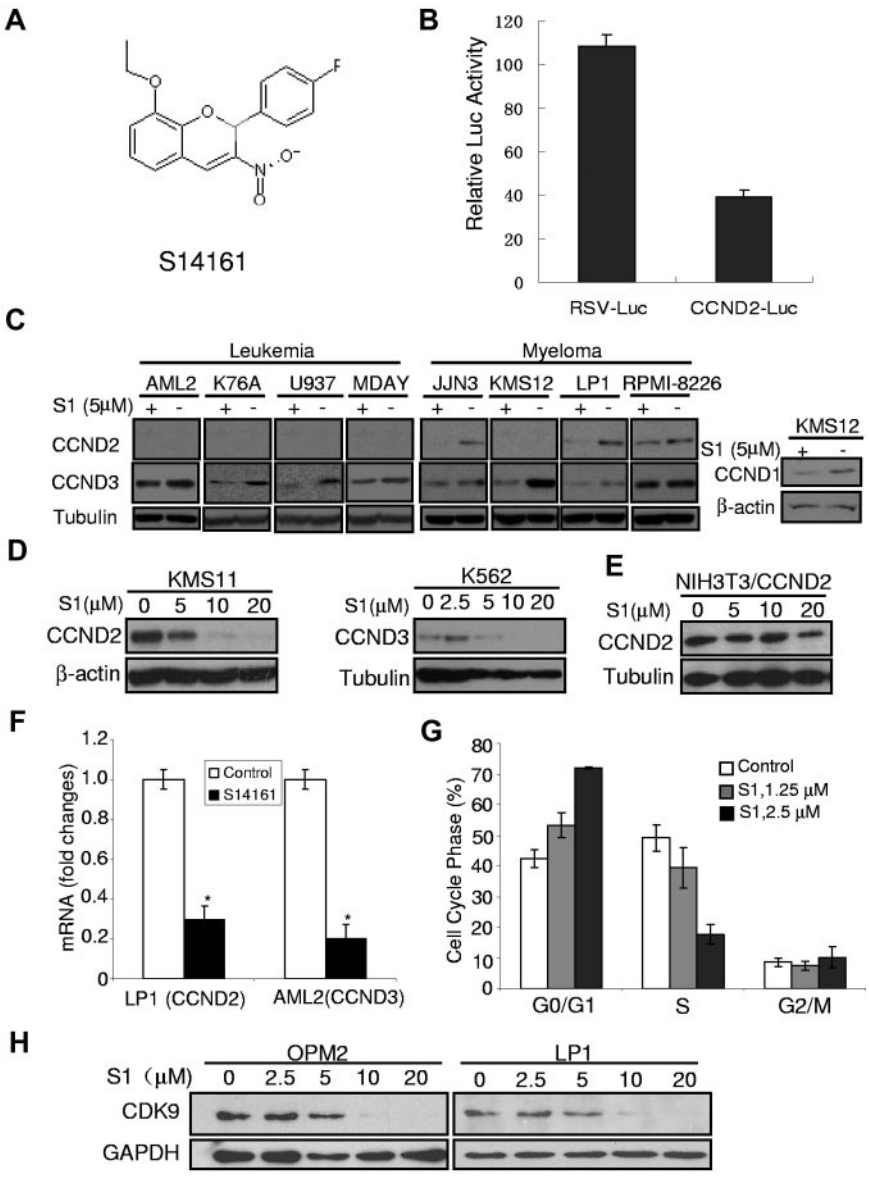

Figure 1. S14161 inhibited D-cyclin expression. (A) The chemical structure of S14161. (B) S14161 inhibited cyclin D2 promoter transactivation. NIH3T3 cells were first transfected with pRSV.Luc and pCCD2.Luc, respectively. Twenty-four hours later, cells were treated with S14161 for 20 hours, followed by performance of a luciferase activity assay as described in "Luciferase assay." Luc indicates luciferase; RSV, Rous sarcoma virus promoter; and CCND2, cyclin D2. (C) Myeloma (JJN3, KMS12, LP1, and RPMI-8226) and leukemia (OCI-AML2, K76A, U937, MDAY) cells were treated with 5μM S14161 (S1) or vehicle for 24 hours. After incubation, cells were harvested and total proteins isolated. Expression of cyclin D1 (CCND1), cyclin D2 (CCND2), cyclin D3 (CCND3), β-actin, and tubulin was measured by immunoblotting. (D) KMS11 and K562 cells were treated with increasing concentrations of S1 for 24 hours. After incubation, cells were harvested and total proteins isolated. Expression of CCND2, CCND3, β-actin, and tubulin was measured by immunoblotting. (E) NIH3T3 cells were transfected with pcDNA3.1-CCND2 (under control of the cytomegalovirus promoter), followed by S1 treatment at indicated concentrations for 24 hours. Cells were harvested for CCND2 expression analysis. Tubulin was used as a loading control. (F) LP1 and AML2 cells were treated with 5μM S1 for 24 hours, and total mRNA was isolated. CCND2 (from LP1) and CCND3 (from AML2) expression was measured relative to 18S RNA by real-time reverse-transcription PCR. Data represent the mean ± SD percentage of D-cyclin expression relative to controls ($^{\Delta\Delta}$CT normalization; n = 3). (G) KMS11 cells were treated with increasing concentrations of S1. Twenty-four hours after incubation, cell cycle was measured by propidium iodide staining and flow cytometry. Data represent the mean ± SD percentage of cells at phases of the cell cycle (n = 3). A representative experiment is shown. (H) Myeloma cells OPM2 and LP1 were treated with S1 at indicated concentrations for 24 hours followed by cell lysates and immunoblotting assay against human CDK9–specific antibody. GAPDH was used as a loading control.

S14161 arrests cells at the G_1 phase of the cell cycle

D-cyclins are required for cell proliferation and entry to the S phase of the cell cycle, and decreasing D-cyclin expression is associated with G_1 arrest.[18-20] Because S14161 decreased levels of D-cyclins, we tested the effects of S14161 on cell-cycle progression. Myeloma and leukemia cells were treated with increasing concentrations of S14161, and the percentage of cells at different phases of the cell cycle was measured by propidium iodide staining and flow cytometry. Consistent with its effect on D-cyclin gene and protein expression, S14161 arrested cells at the G_0/G_1 phase (Figure 1G) in a dose-dependent manner.

S14161 induces blood cancer cell apoptosis

Reductions in D-cyclins and G_0/G_1 arrest can induce apoptosis in malignant cells.[21,22] Therefore, we tested the effects of S14161 on the viability of myeloma and leukemia cells. A panel of cell lines was treated with increasing concentrations of S14161, and cell growth and viability were measured by the MTS assay 24, 48, and 72 hours after treatment. S14161 reduced the proliferation and viability of cell lines in a time- and dose-dependent manner. For example, at 72 hours after treatment, S14161 induced cell death in 6 of 7 myeloma and 6 of 7 leukemia cell lines with a half-maximal inhibitory concentration (IC_{50}) < 10μM (supplemental Figure 1, available on the *Blood* Web site; see the Supplemental Materials link at the top of the online article). Cell death and apoptosis were confirmed by annexin V–fluorescein isothiocyanate staining (Figure 2B). Mechanistically, cell death induced by S14161 was associated with activation of caspase-3, caspase-9, and poly(ADP ribose) polymerase (Figure 2C). Cell death induced by S14161 was also associated with decreased levels of antiapoptotic proteins such as Bcl-2 and Mcl-1 and increased levels of proapoptotic proteins such as Bim (Figure 2D).

We also evaluated the effects of S14161 on the viability of primary acute myeloid leukemia and normal hematopoietic cells. S14161 reduced the growth and viability of 4 of 5 primary acute myeloid leukemia samples with an IC_{50} < 10μM (Figure 2A). In

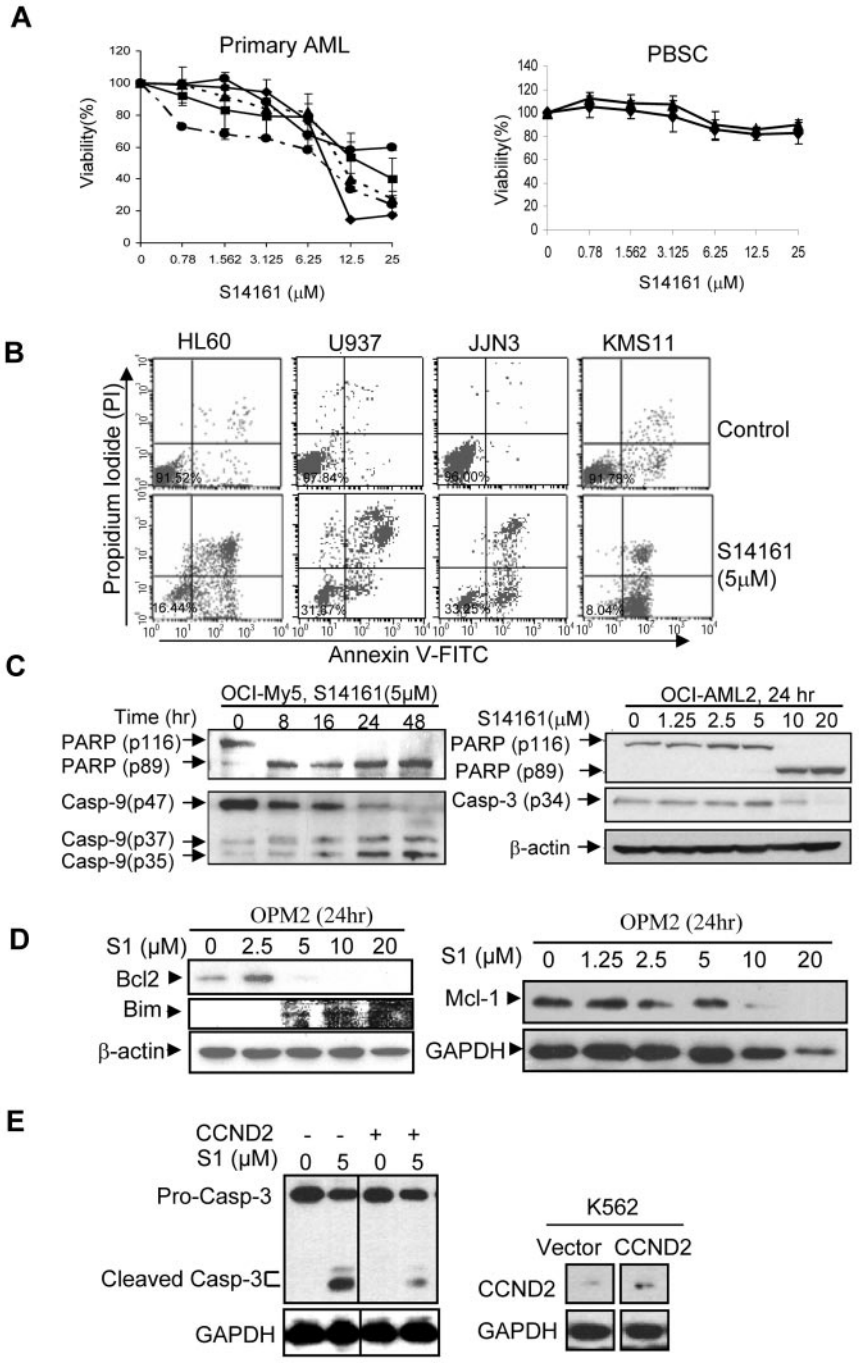

Figure 2. S14161 induced cell death and apoptosis in myeloma and leukemia cells and primary patient samples. (A) Acute myeloid leukemia (AML) patient samples (n = 5) and normal hematopoietic cells (peripheral blood stem cells [PBSC]) were treated with increasing concentrations of S14161. Seventy-two hours after incubation, cell growth and viability were measured by the MTS assay. Data represent the mean percentage of viable cells ± SD from experiments performed in triplicate. (B) Leukemia (HL60 and U937) and myeloma (JJN3 and KMS11) cells were treated with S1 (5μM) or vehicle control. Twenty-four hours after treatment, apoptosis was measured by annexin V staining. A representative experiment is shown. FITC indicates fluorescein isothiocyanate. (C) Myeloma cells OCI-My5 (left) were incubated with 5μM S1 for the indicated time. After incubation, cells were harvested and total proteins isolated. Cleavage of poly(ADP ribose) polymerase (PARP) and caspase-9 (Casp-9) was measured by immunoblotting. Right, OCI-AML2 cells were treated for 24 hours at indicated concentrations, followed by evaluation of PARP and caspase-3 (Casp-3). (D) Myeloma (OPM2) cells were treated with increasing concentrations of S14161 (S1) for 24 hours. After incubation, cells were harvested and total proteins isolated. Expression of Bim, Bcl-2, Mcl-1, and loading controls β-actin and GAPDH was measured by immunoblotting. (E) Leukemia cells K562 were transfected with cyclin D2 with nanoparticles used as vectors (IR). Twenty-four hours later, cells were harvested for cyclin D2 (CCND2) evaluation (right) or further treated with S14161 (S1) for 24 hours followed by caspase-3 (Casp-3) activation analysis with caspase-3 specific antibody. Both pro-Casp-3 and cleaved Casp-3 fragments were detected. GAPDH was used as a loading control.

contrast, it was less toxic to normal hematopoietic cells, with an IC_{20} (concentration of 20% inhibition) > 25μM (Figure 2A).

To further examine whether S14161-induced cell apoptosis was associated with cyclin D expression, we transduced cyclin D2 plasmid or empty vector into LP1 cells, followed by apoptosis analysis after 24 hours of incubation. LP1 cells overexpressing cyclin D2 became resistant to S14161 (supplemental Figure 2). S14161 induced 39% apoptosis in native LP1 cells within 24 hours, but this effect was partially abolished by overexpression of cyclin D2; only 25% of cells underwent apoptosis after cyclin D2 transduction (supplemental Figure 2). To confirm this, we transduced cyclin D2 plasmids into K562 cells using the nanovector IR. Cyclin D2 was well introduced into K562 cells (Figure 2E right), and the expression of cyclin D2 enabled K562 cells to resist apoptosis induced by S14161, as evidenced by caspase-3 activation, which was reduced in cyclin D2–transduced cells (Figure 2E left).

To examine whether caspases are important for cyclin D down-regulation, we pretreated K562 and LP1 cells with the pan-caspase inhibitor Z-VAD-FMK (R&D Systems), followed by S14161 treatment. Results indicated that the decrease in cyclin D caused by S14161 was not prevented by Z-VAD-FMK (supplemental Figure 3), which suggests that cyclin D down-regulation by S14161 is independent of caspase activation. In contrast, cyclin D overexpression could partially abolish caspase-3 activation (Figure 2E). Thus, cyclin D was functionally important for S14161-induced blood cancer cell apoptosis.

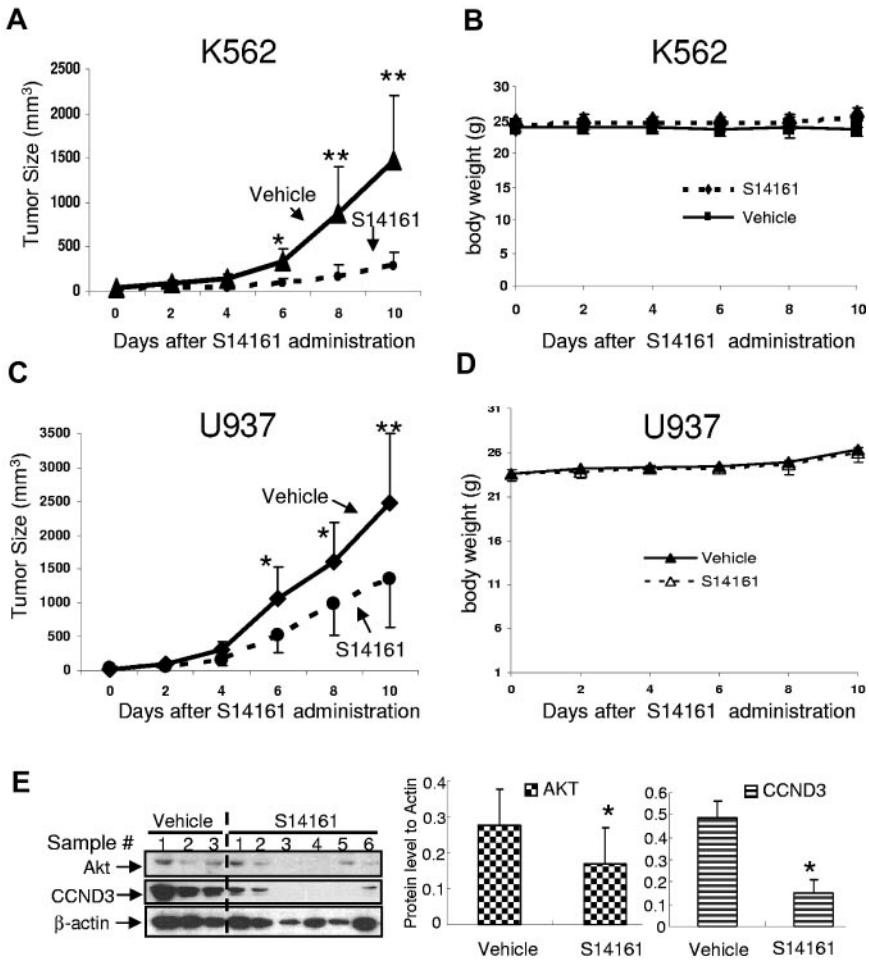

Figure 3. S14161 delayed the tumor growth in leukemia xenografts. K562 (A,B) and U937 (C,D) leukemia cells were injected subcutaneously into SCID mice. When the tumors were palpable, mice were treated with S14161 (100 mg/kg) or vehicle control intraperitoneally for 10 days (n = 10 per group). Tumor growth (A,C) and body weight (B,D) were monitored every other day. Data represent the mean ± SD of a representative experiment. *$P < .05$, **$P < .001$ by Student *t* test. (E) Tumor samples from U937 xenograft mice models after 10 days of treatment with S14161 were excised. Total AKT and cyclin D3 (CCND3) were evaluated by immunoblotting with specific antibodies (left). Relative expression of AKT (middle) and CCND3 (right) was quantitated by densitometric analysis based on the immunoblotting assay result (left). *Significant difference ($P < .01$) between vehicle control and S14161 treatment.

S14161 inhibits tumor growth in leukemia xenograft models

Given the ability of S14161 to induce apoptosis and reduce D-cyclin expression, we evaluated its efficacy in vivo. SCID mice were injected subcutaneously with K562 human chronic leukemia cells or U937 human acute leukemia cells. Mice were treated with S14161 (100 $mg \cdot kg^{-1} \cdot d^{-1}$) or vehicle control intraperitoneally for 10 days. Tumor growth was monitored every other day. Treatment with S14161 delayed tumor growth by up to 90% compared with vehicle control in K562 models (Figure 3A) without evidence of gross organ toxicity or weight loss (Figure 3B). S14161 also markedly delayed tumor growth in mice implanted with U937 cells (Figure 3C) but had no effect on mouse weight over the period of the experiment (Figure 3D). Of note, in our acute toxicity experiment, no weight loss or other toxic changes were observed in mice treated with 500 mg/kg/d for 2 weeks (data not shown). Our previous study indicated that S14161 decreased cyclin D expression in both leukemia and myeloma cells, thus inducing cell apoptosis. To determine whether S14161 could decrease cyclin D in tumor species, thus inhibiting tumor growth, we analyzed cyclin D protein levels in U937 xenografts after 10 days of treatment. Western blotting analyses indicated that S14161 significantly decreased cyclin D3 expression in tumors compared with those treated with vehicle. More than 70% of cyclin D3 was decreased in S14161-treated mice (Figure 3E).

S14161-induced apoptosis occurs via the PI3K signaling pathway

S14161 is a novel chemical compound with an unknown mechanism of action, but it down-regulated cyclin D expression on a transcriptional level. Because the PI3K signaling pathway is important in the regulation of transcription and the expression of D cyclins,[19,20] we tested whether S14161 could inhibit the PI3K signaling pathway and whether this inhibition was functionally important with regard to its effects on D-cyclin expression and cell viability. Various leukemia and myeloma cells were pretreated with S14161, followed by IGF1 stimulation. IGF1 increased levels of phospho-AKT in both myeloma and leukemia cells, but such activation of AKT was abolished by S14161 and by LY294002, the classic PI3K inhibitor (Figure 4A). Of note, inhibition of the PI3K signaling pathway by S14161 could be detected within 1 hour after addition of the compound (Figure 4B). In addition, after an overnight incubation, S14161 decreased basal levels of phospho-AKT (Figure 4C). Similar to the effects of S14161, LY294002 also down-regulated cyclin D2, arrested cells at the G_1 phase of the cell cycle (supplemental Figure 4), and activated caspase-9 and poly-(ADP-ribose) polymerase cleavage.[21] In addition, S14161 decreased total AKT expression, which was further confirmed in leukemia xenografts treated with S14161 for 10 days (Figure 3E), in which S14161 down-regulated total AKT expression along with cyclin D.

To further understand the relevance of S14161-induced apoptosis and PI3K/AKT/cyclin D, we compared the effects of S14161 on cell apoptosis and cyclin D expression in both KMS11 (which expressed constitutively active AKT) and U266 (without active AKT) cells.[22] As shown in Figure 4D, KMS11 cells that expressed phospho-AKT were more sensitive than U266 cells in which no activated AKT was observed. Consistent with our hypothesis, S14161 displayed no effects on cyclin D expression in U266 cells

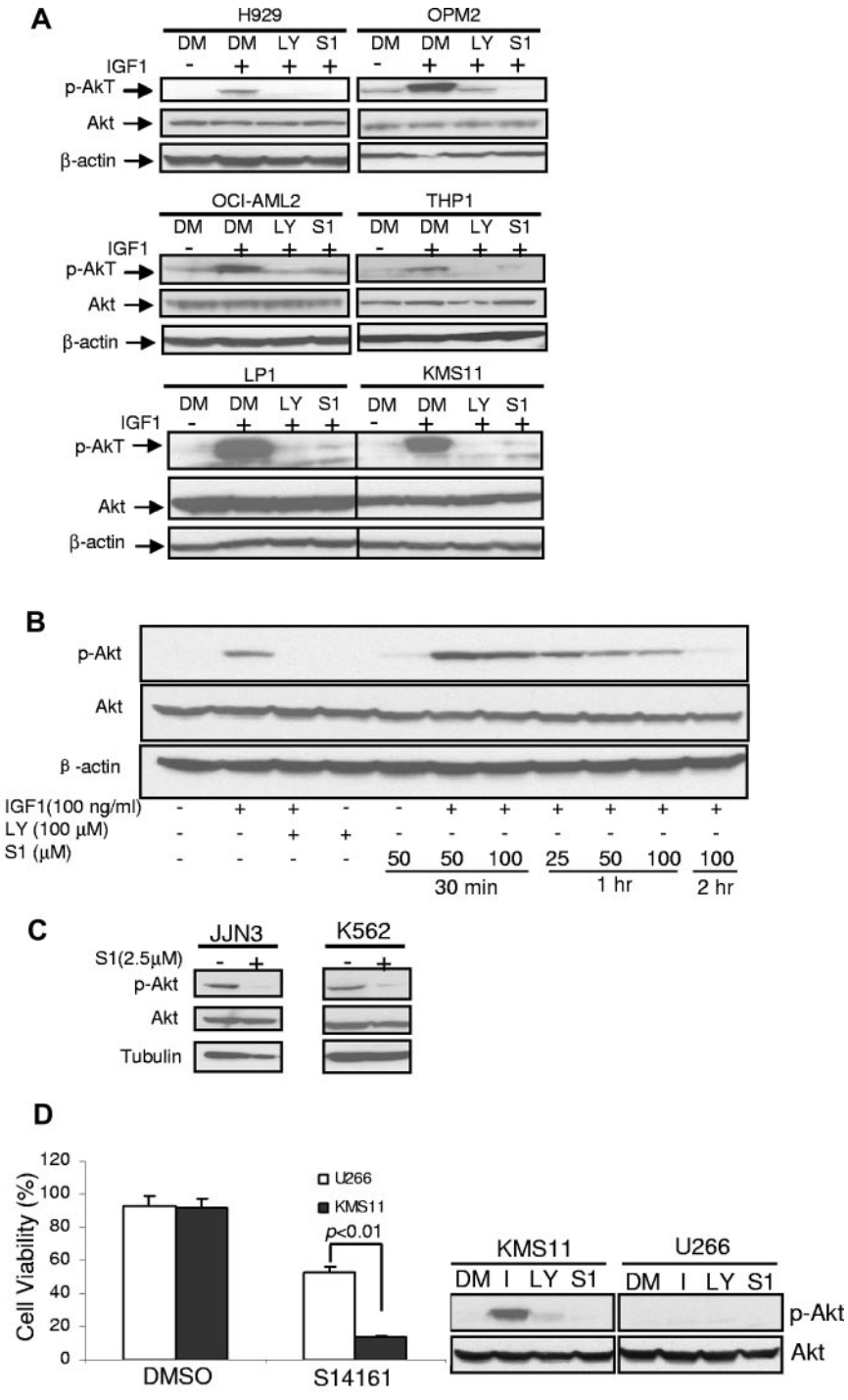

Figure 4. S14161 inhibited the PI3K signaling pathway. (A) Myeloma (H929, OPM2, LP1, and KMS11) and leukemia (OCI-AML2 and THP1) cells were starved overnight and then treated with S14161 (S1; 100μM for 2 hours), LY294002 (LY; 100μM for 30 minutes), or DMSO (DM; 2 hours), followed by 100 ng/mL IGF1 for 10 minutes. After incubation, cells were harvested and total proteins isolated. Expression of AKT, phospho-AKT (p-AKT), and β-actin was measured by immunoblotting. (B) KMS11 cells were treated with increasing concentrations of S1 for 0.5, 1, or 2 hours, followed by IGF1 stimulation. Cells were then harvested and total proteins isolated. Expression of AKT, p-AKT, and β-actin was measured by immunoblotting. (C) JJN3 and K562 cells were treated with S1 (2.5μM) or DMSO control for 24 hours. After incubation, cells were harvested and total proteins isolated. Expression of AKT, p-AKT, and β-actin was measured by immunoblotting. (D) Phosphorylated AKT was important for S14161-induced cell death. KMS11 and U266 cells were treated with increasing concentrations of 5μM S1 for 24 hours, followed by apoptosis analysis with annexin V staining. At the same time, KMS11 and U266 cells were subjected to AKT phosphorylation analysis.

(data not shown) but down-regulated cyclin D2 in KMS11 cells (Figure 1D). Thus, S14161 induced cell apoptosis via the PI3K/AKT/cyclin D pathway.

S14161 blocks AKT translocation to cytoplasmic membrane

In the PI3K/AKT cell signaling cascade, PI3K activation leads to the production of $PI(3,4,5)P_3$, which recruits AKT and PDK1 to the plasma membrane, where AKT is phosphorylated by PDK1.[23,24] As an alternate approach to examine the effects of S14161 on the PI3K signaling pathway, we visualized changes in levels and localization of phospho-AKT using confocal microscopy. OPM2 myeloma cells were treated with S14161, LY294002, or DMSO control with or without IGF1 to stimulate the PI3K pathway. After treatment, levels and localization of total and phospho-AKT were visualized on a confocal microscope (Figure 5). Consistent with previous reports,[25] stimulation of the PI3K pathway with IGF1 induced the translocation of AKT to the plasma membrane and its phosphorylation (Figure 5A,D). Moreover, IGF1 increased the translocation of AKT from the nucleus to the cytoplasm as described previously (Figure 5D).[26] In keeping with its ability to inhibit the PI3K signaling pathway, S14161 decreased levels of phospho-AKT and prevented its membrane localization after IGF1 stimulation (Figure

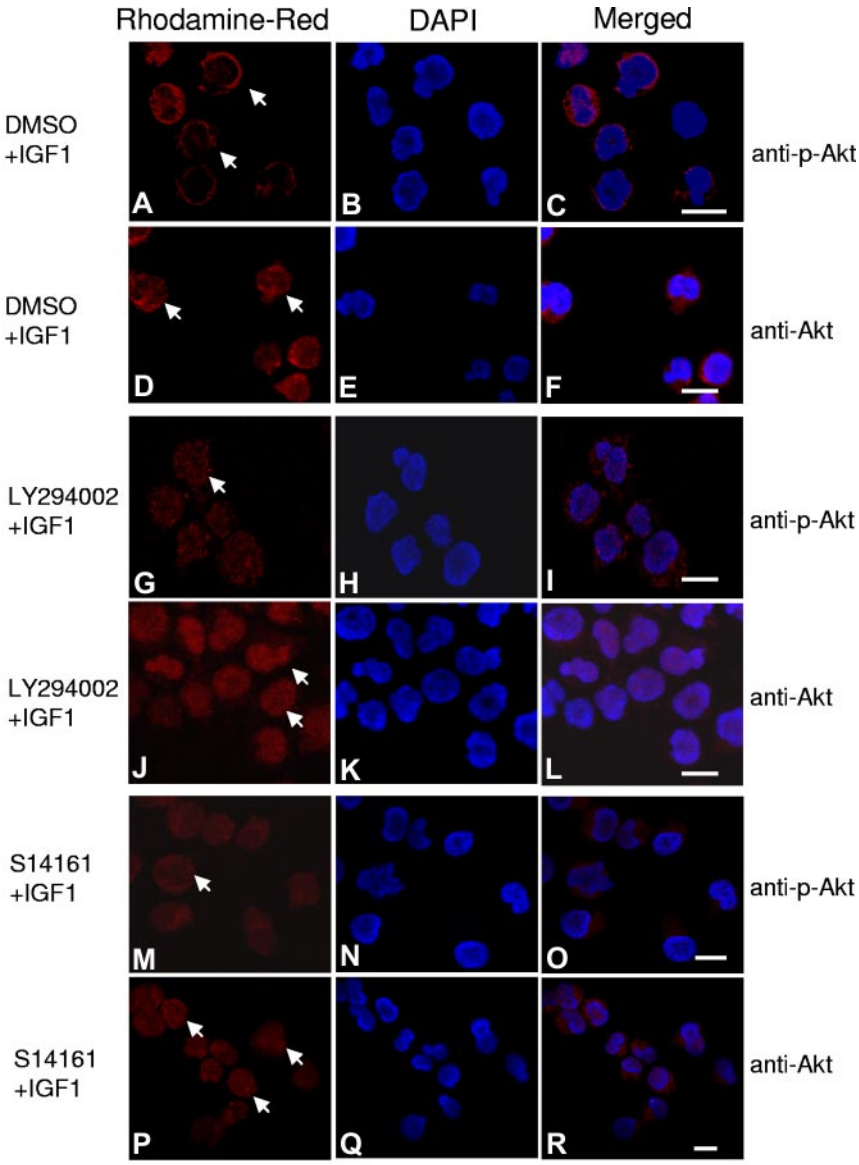

Figure 5. S14161 inhibited phospho-AKT translocation and accumulation at the cytoplasmic membrane. OPM2 myeloma cells were starved overnight, followed by treatment with S14161 (100μM for 1 hour), LY294002 (100μM for 30 minutes), or DMSO control for 1 hour. Cells were then treated with 100 ng/mL IGF1 for 10 minutes. Cells were fixed and stained with antibodies against AKT or phospho-AKT (p-AKT) and DAPI (4,6 diamidino-2-phenylindole) as described in "Immunofluorescence assay." Red indicates AKT or p-AKT; blue, nuclei. (A-C) Phospho-AKT (arrows) stimulated by IGF; (D-F) total AKT translocated to the plasma membrane after IGF1 treatment; (G-I) Phospho-AKT inhibited by LY294002; (J-L) total AKT located in the nuclei after LY294002 treatment; (M-O) phospho-AKT inhibited by S14161; and (P-R) total AKT was restricted to the nuclei after S14161 treatment.

5M). However, S14161 did not change the abundance or localization of total AKT during the observation period (Figure 5P).

S14161 inhibits PI3K enzymatic activity

Given the effects of S14161 on the PI3K signaling pathway, we examined its ability to inhibit recombinant PI3K enzymes (Millipore) in a cell-free enzymatic assay. S14161 inhibited the activities of class I PI3K-α, -β, -γ, and -δ with similar efficacy (Figure 6A). In contrast, S14161 was less effective in inhibiting the PI3K-associated enzymes PDK1, mTOR, and the DNA-dependent protein kinase catalytic subunit (DNA-PKcs), with less than 20% inhibition at a concentration of 300μM (data not shown). Likewise, S14161 did not inhibit AKT1, AKT2, or AKT3 at a concentration up to 300μM (data not shown).

The PI3Ks used above were recombinant; thus, to examine the effects of S14161 on endogenous PI3K activity, we used anti-p85 antibody to enrich and purify PI3Ks derived from leukemia cell line K562 and myeloma cell line LP1 and then analyzed the activity of these PI3Ks using ELISA methods. The inhibitory patterns of S14161 on endogenous PI3Ks were similar to those from recombinant ones at similar IC_{50}s (data not shown).

These studies suggested that S14161 inhibited PI3K activity in vivo in terms of AKT phosphorylation. To evaluate the direct inhibition of S14161 on PI3K in vivo, we treated myeloma OPM2 cells with S14161 for 2 hours, followed by IGF1 stimulation. These cells were then lysed and used for PI3K immunoprecipitation before being subjected to activity analysis. As expected, S14161 inhibited PI3K activity and decreased the production of $PI(3,4,5)P_3$, as shown in Figure 6B. Thus, S14161 could directly inhibit PI3K activity in vivo.

S14161 down-regulates cyclin D expression via PI3K/AKT pathway

Our studies indicated S14161 decreased cyclin D expression and interrupted the PI3K/AKT pathway by direct inhibition on PI3K activity (Figures 4 and 6) and AKT translocation between cellular compartments (Figure 5). Previous studies have established that cyclin D expression is regulated by PI3K/AKT.[21] To demonstrate inhibition of cyclin D transactivation by S14161 via the PI3K/AKT pathway, we examined the association of cyclin D and AKT expression patterns using myeloma KMS11 as a representative. As shown in supplemental Figure 5A, cyclin D2 expression remained

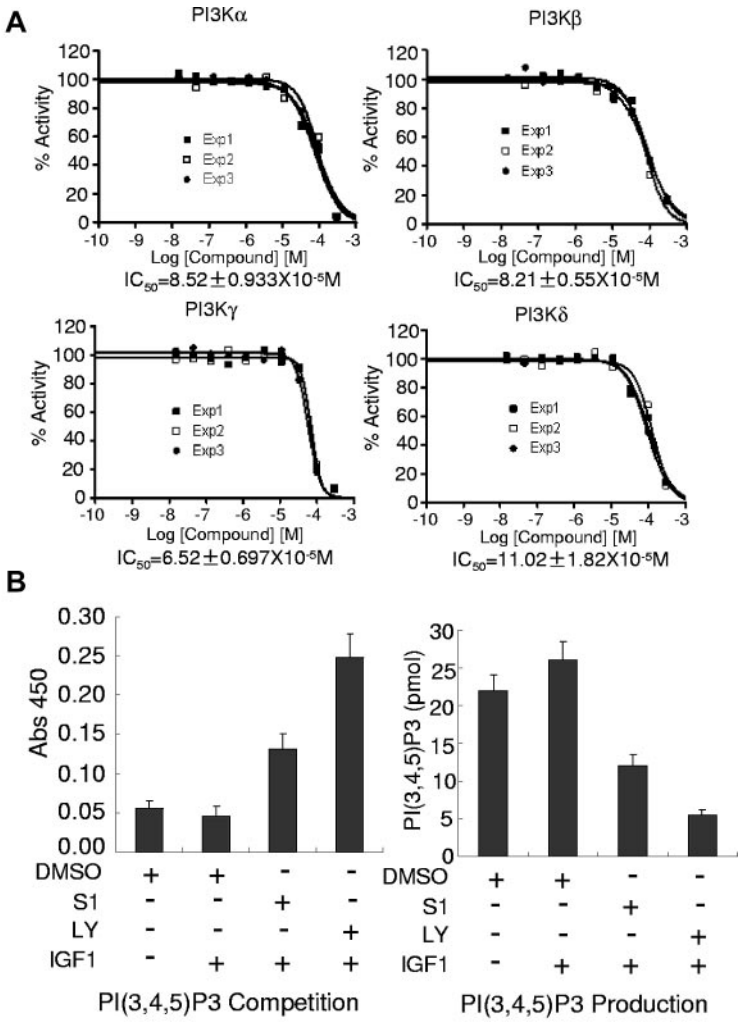

Figure 6. S14161 inhibited PI3K activity. (A) PI3K activity analysis in an in vitro cell-free system. Increasing concentrations of S14161 were incubated with the PI3K isoforms α, β, γ, and δ, respectively. Activity of each kinase was determined with HotSpot technology as described in "Kinase activity in cell-free assay." The results of 3 independent experiments are presented. Exp1, Exp2, and Exp3 indicate experiments 1, 2, and 3, respectively. (B) PI3K activity analysis after S14161 treatment in vivo. OPM2 cells were treated with S14161. Cell lysates were prepared and used for PI3K immunoprecipitation. PI3K activity was analyzed by ELISA as described in "Immunoprecipitation of P13K and P13K activity evaluation by ELISA." Abs 450, absorbance at 450 nm of wavelength; S1, S14161; and LY, LY294002.

at a high level, and its half-life was not measurable in the intact myeloma cell line KMS11; however, it was shortened by S14161. AKT became undetectable at 1.5-2 hours after S14161 treatment; cyclin D2 decreased accordingly, and this change remained at 1 hour (between 1 and 2 hours; supplemental Figure 5B). Interestingly, both AKT and cyclin D2 recovered slightly at 4 hours of treatment and then steadily decreased by S14161 in a time-dependent manner (supplemental Figure 5B). This type of down-regulation of AKT and cyclin D by S14161 was also concentration dependent (supplemental Figure 5C). Given the results of the studies discussed above, especially the S14161-induced concomitant decrease of AKT and cyclin D (supplemental Figure 5), PI3K activity inhibition (Figures 4 and 6), and the interruption of AKT translocation (Figure 5), and the well-established link that shows that PI3K/AKT regulates cyclin D transcription,[21] we concluded that S14161 down-regulated cyclin D by interfering with PI3K/AKT signals.

Evaluation of S14161 analogues

To assess the relationship between inhibition of PI3K signaling, decreased D-cyclin expression, and cell death, we evaluated a series of chromene-containing compounds structurally related to S14161 (Figure 7A). Similar to the effects of S14161, the highly structurally related compound 8-methoxy-2-(4-fluorophenyl)-3-nitro-2H-chromene (S14147) inhibited accumulation of phospho-AKT after IGF1 stimulation, decreased D-cyclin expression, and induced cell death in KMS11 myeloma cells (Figure 7B-D). In contrast, other related compounds did not decrease cyclin D expression or prevent AKT phosphorylation after IGF1 stimulation (Figure 7B-C). These inactive analogues were not toxic to myeloma cells (Figure 7D). Thus, the association of S14161-induced cell apoptosis and inhibition of cyclin D via the PI3K/AKT pathway was established. S14161 repressed the transactivation of D-cyclins by interfering with the PI3K/AKT pathway, thus inducing myeloma and leukemia cell apoptosis.

Discussion

D-cyclins regulate the cell cycle by acting in a complex with CDKs to promote phosphorylation of the retinoblastoma protein and initiate cellular progression from the G_1 to the S phase.[1] Aberrant expression of D-cyclins is found almost universally in multiple myeloma, in which they stimulate progression of the cell cycle and promote cell growth and proliferation.[27] Therefore, molecules that decrease D-cyclin expression would be useful chemical probes to better understand this biological pathway and its relation to malignancy. In the present study, we conducted a chemical screening for compounds and identified the novel compound S14161, which inhibited transactivation of the cyclin D2 promoter

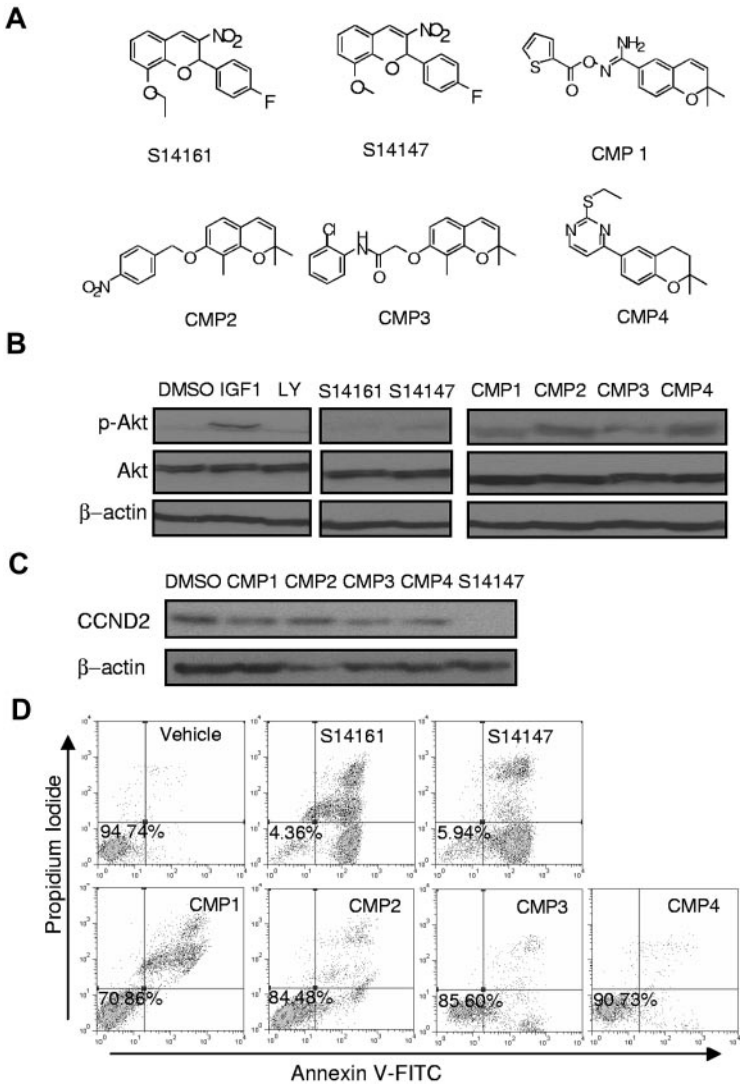

Figure 7. Evaluation of S14161 analogues. (A) The chemical structures of S14161, S14147, and compounds 1-4 (CMP1, CMP2, CMP3, and CMP4). (B) Starved KMS11 cells were treated by S14161, its analogs, or DMSO for 2 hours followed by 100 ng/mL IGF1 for 10 minutes. After incubation, cells were harvested and total proteins isolated. Expression of AKT, phospho-AKT (p-AKT), and β-actin was measured by immunoblotting. LY indicates LY294002. (C) KMS11 cells were treated for 24 hours with compounds 1-4 or S14147 or vehicle DMSO (each at 10μM). After incubation, cells were harvested and total proteins isolated. Expression of cyclin D2 (CCND2) and β-actin was measured by immunoblotting. (D) JJN3 cells were treated with 10μM S14161, S14147, compounds 1-4, or buffer control for 24 hours. After incubation, apoptosis was measured by annexin V–fluorescein isothiocyanate (FITC) and propidium iodide staining. A representative experiment is shown.

and induced cell death in myeloma and leukemia cell lines and primary patient samples. Moreover, it delayed tumor growth in mouse models of leukemia. Mechanistically, S14161-induced cell death and tumor growth delay were due to its inhibition of D-cyclin expression, as demonstrated by its inhibition of cyclin D transcription and cyclin D2 promoter transactivation rather than cyclin D2 translation and posttranslational modification. The inhibition by S14161 of cyclin D transcription crosses a variety of transforming events, including c-maf overexpression, FGFR3 translocation, and cyclin D1 translocation, which suggests that S14161 could interfere with other signaling pathways that overcome or bypass these events associated with cyclin D expression. Among these signals, PI3K/AKT is one of the most significant.

The PI3K/AKT signaling pathway plays an important role in various cell activities, including cell proliferation and antiapoptosis. The link between PI3K and D-cyclin transcription has been established in previous studies in which inhibition of PI3K/AKT led to decreased cyclin D expression.[19,20] For example, activation of PI3K signaling increased transcription of cyclin D1 mRNA by regulating JunD–nuclear factor κB–mediated activation of the cyclin D1 promoter.[28] That S14161 inhibits PI3K activity was observed in both cellular and cell-free enzymatic assays by direct evaluation of $PI(3,4,5)P_3$ production (Figure 6), AKT translocation between cellular compartments (Figure 5), and AKT phosphorylation (Figure 4). The ability of S14161 to overcome a broad spectrum of transforming events via the PI3K pathway indicates that this PI3K inhibitor can reduce D-cyclin expression independent of specific transforming pathways and that S14161 is biologically important to induce apoptosis in both leukemia and myeloma cells.

PI3K/AKT signaling is frequently aberrant in leukemia and myeloma cells.[29-31] For example, PTEN, the phosphatase that reverses $PI(3,4,5)P_3$ to $PI(4,5)P_2$, is mutated or deleted in OPM2,[20] U937,[29] and THP-1 cells.[30] In addition, hypermethylation of the PTEN promoter was detected in the OCI-AML2, HL-60, U937, Nalm-6, Raji, and KG-1a cell lines.[32] PI3K and AKT are overactivated in most myeloma and leukemia cells,[33] such as APL[34] and T-ALL.[35,36] These changes lead to aberrant PI3K/AKT signals, thus increasing cellular proliferation and chemoresistance.[37] Consistent with these effects, increased activation of the PI3K pathway is prognostically important in patients with myeloma and leukemias.[14,38] For example, increased levels of phospho-AKT (Ser473) are associated with worse overall survival and worse response to reinduction chemotherapy in patients with acute myeloid leukemia.[39] AKT phosphorylation is critical for S14161-induced blood cancer cell apoptosis, because U266 lacking a phosphorylated AKT is resistant to S14161-induced cell death. This interruption of S14161 in the PI3K/AKT signaling pathway in leukemia and

myeloma cells will lead to decreased proliferation, delayed tumor growth, and increased chemosensitivity of these malignant cancer cells.

The PI3K superfamily can be divided into 4 different classes (class I, II, III, and IV) based on primary structure, regulation, and in vitro substrate specificity. LY294002, one of the classic PI3K inhibitors, inhibits both class I and class IV PI3Ks, as well as AKT and glycogen synthase kinase, with similar potency. LY294002 displays activity in vitro and in vivo[40]; however, its toxicity renders it unsuitable for clinical use. Although we cannot exclude additional targets for S14161 that influence its ability to decrease D-cyclins and induce cell death, S14161 inhibited the activity of all 4 isoforms of the PI3K class I family, including PI3K-α, -β, -γ, and -δ, in enzymatic assays (Figure 6). In contrast, it had no effects on class IV enzymes, such as mTOR and DNA-PKcs, or on other kinases such as AKT-1, -2, or -3 or PDK1 in a similar enzymatic assay system. Thus, this specific inhibition of S14161 on PI3Ks is probably responsible for its reduced toxicity; furthermore, S14161 displayed no gross toxicity at concentrations up to 500 mg/kg in mice by intraperitoneal administration. All of these characteristics render S14161 as a drug candidate.

Although displaying less potency than LY294002 in terms of inhibition of PI3K activity in an in vitro cell-free assay, S14161 was more potent or at least comparably potent in terms of induction of apoptosis and inhibition of PI3K activity in cells (Figures 4 and 6). One of the possible explanations for this result is that S14161 is metabolized and activated in cells and that its cellular metabolites are more active than parental S14161. Therefore, it would be of interest and of importance to further evaluate the metabolism of S14161, and this pharmacophore might be further developed to make more potent compounds.

Through this work, we have identified a novel chemical compound that inhibits D-cyclin transactivation via inhibition of the PI3K pathway. These results support PI3K inhibition as a strategy to overcome the chemoresistance conferred by dysregulation of D-cyclins in myeloma and leukemia.

Acknowledgments

We thank Pricilla De Luca for her editing of the manuscript.

This work was supported by the Ontario Institute for Cancer Research (OICR) of Canada, by Jiangsu Provincial Nature and Science Foundation (grant No. BK2010218) of China, and by Chinese National Key Projects (project 973, grants 2011CB933501 and 2011CB933503). A.D.S. is a Clinical Research Scholar of the Leukemia & Lymphoma Society.

Authorship

Contribution: X.M. and A.D.S. designed the research, analyzed data, performed research, and wrote the manuscript; B.C., T.E.W., R.H., J.T., X.W., W.W., J.L., Y.J., W.S., P.A.S., N.M., and A.D. performed research and analyzed data; and M.F.M., R.A.B., and J.W. analyzed data.

Conflict-of-interest disclosure: The authors declare no competing financial interests.

Correspondence: Xinliang Mao, MD, PhD, Cyrus Tang Hematology Center, Soochow University, 199 Ren Ai Rd, Suzhou Industrial Park, Suzhou, China 215123; e-mail: xinliangmao@suda.edu.cn.

References

1. Sherr CJ. Cancer cell cycles. *Science.* 1996; 274(5293):1672-1677.
2. Ely S, Di Liberto M, Niesvizky R, et al. Mutually exclusive cyclin-dependent kinase 4/cyclin D1 and cyclin-dependent kinase 6/cyclin D2 pairing inactivates retinoblastoma protein and promotes cell cycle dysregulation in multiple myeloma. *Cancer Res.* 2005;65(24):11345-11353.
3. Sasaki Y, Jensen CT, Karlsson S, Jacobsen SE. Enforced expression of cyclin D2 enhances the proliferative potential of myeloid progenitors, accelerates in vivo myeloid reconstitution, and promotes rescue of mice from lethal myeloablation. *Blood.* 2004;104(4):986-992.
4. Yata K, Sadahira Y, Otsuki T, et al. Cell cycle analysis and expression of cell cycle regulator genes in myeloma cells overexpressing cyclin D1. *Br J Haematol.* 2001;114(3):591-599.
5. Hochhauser D, Schnieders B, Ercikan-Abali E, et al. Effect of cyclin D1 overexpression on drug sensitivity in a human fibrosarcoma cell line. *J Natl Cancer Inst.* 1996;88(18):1269-1275.
6. Sarfaraz S, Afaq F, Adhami VM, Malik A, Mukhtar H. Cannabinoid receptor agonist-induced apoptosis of human prostate cancer cells LNCaP proceeds through sustained activation of ERK1/2 leading to G1 cell cycle arrest. *J Biol Chem.* 2006;281(51): 39480-39491.
7. Baughn LB, Di Liberto M, Wu K, et al. A novel orally active small molecule potently induces G1 arrest in primary myeloma cells and prevents tumor growth by specific inhibition of cyclin-dependent kinase 4/6. *Cancer Res.* 2006;66(15): 7661-7667.
8. Mantena SK, Sharma SD, Katiyar SK. Berberine inhibits growth, induces G1 arrest and apoptosis in human epidermoid carcinoma A431 cells by regulating Cdki-Cdk-cyclin cascade, disruption of mitochondrial membrane potential and cleavage of caspase 3 and PARP. *Carcinogenesis.* 2006; 27(10):2018-2027.
9. Bergsagel PL, Kuehl WM, Zhan F, Sawyer J, Barlogie B, Shaughnessy J Jr. Cyclin D dysregulation: an early and unifying pathogenic event in multiple myeloma. *Blood.* 2005;106(1):296-303.
10. Valk PJ, Verhaak RG, Beijen MA, et al. Prognostically useful gene-expression profiles in acute myeloid leukemia. *N Engl J Med.* 2004;350(16): 1617-1628.
11. Hanamura I, Huang Y, Zhan F, Barlogie B, Shaughnessy J. Prognostic value of cyclin D2 mRNA expression in newly diagnosed multiple myeloma treated with high-dose chemotherapy and tandem autologous stem cell transplantations. *Leukemia.* 2006;20(7):1288-1290.
12. Mao X, Stewart AK, Hurren R, et al. A chemical biology screen identifies glucocorticoids that regulate c-maf expression by increasing its proteasomal degradation through up-regulation of ubiquitin. *Blood.* 2007;110(12):4047-4054.
13. Mao X, Zhu X, Hurren R, Ezzat S, Schimmer AD. Dexamethasone increases ubiquitin transcription through an SP-1 dependent mechanism in multiple myeloma cells. *Leuk Res.* 2008;32(9):1480-1482.
14. Mao X, Liang SB, Hurren R, et al. Cyproheptadine displays preclinical activity in myeloma and leukemia. *Blood.* 2008;112(3):760-769.
15. Tiedemann RE, Mao X, Shi CX, et al. Identification of kinetin riboside as a repressor of CCND1 and CCND2 with preclinical antimyeloma activity. *J Clin Invest.* 2008;118(5):1750-1764.
16. Carter BZ, Gronda M, Wang Z, et al. Small-molecule XIAP inhibitors derepress downstream effector caspases and induce apoptosis of acute myeloid leukemia cells. *Blood.* 2005;105(10):4043-4050.
17. Carlson B, Lahusen T, Singh S, et al. Down-regulation of cyclin D1 by transcriptional repression in MCF-7 human breast carcinoma cells induced by flavopiridol. *Cancer Res.* 1999;59(18): 4634-4641.
18. Chen R, Chubb S, Cheng T, Hawtin RE, Gandhi V, Plunkett W. Responses in mantle cell lymphoma cells to SNS-032 depend on the biological context of each cell line. *Cancer Res.* 2010;70(16): 6587-6597.
19. White PC, Shore AM, Clement M, et al. Regulation of cyclin D2 and the cyclin D2 promoter by protein kinase A and CREB in lymphocytes. *Oncogene.* 2006;25(15):2170-2180.
20. Brennan P, Mehl AM, Jones M, Rowe M. Phosphatidylinositol 3-kinase is essential for the proliferation of lymphoblastoid cells. *Oncogene.* 2002; 21(8):1263-1271.
21. Georgakis GV, Li Y, Rassidakis GZ, Medeiros LJ, Mills GB, Younes A. Inhibition of the phosphatidylinositol-3 kinase/AKT promotes G1 cell cycle arrest and apoptosis in Hodgkin lymphoma. *Br J Haematol.* 2006;132(4):503-511.
22. Zollinger A, Stuhmer T, Chatterjee M, et al. Combined functional and molecular analysis of tumor cell signaling defines 2 distinct myeloma subgroups: AKT-dependent and AKT-independent multiple myeloma. *Blood.* 2008;112(8):3403-3411.
23. Chan TO, Tsichlis PN. PDK2: a complex tail in one AKT. *Sci STKE.* 2001;2001(66):pe1.
24. Harris TK. PDK1 and PKB/AKT: ideal targets for development of new strategies to structure-based drug design. *IUBMB Life.* 2003;55(3):117-126.

25. Meier R, Thelen M, Hemmings BA. Inactivation and dephosphorylation of protein kinase Balpha (PKBalpha) promoted by hyperosmotic stress. *EMBO J.* 1998;17(24):7294-7303.
26. Zhang C, Yang N, Yang CH, et al. S9, a novel anticancer agent, exerts its anti-proliferative activity by interfering with both PI3K-AKT-mTOR signaling and microtubule cytoskeleton. *PLoS ONE.* 2009;4(3):e4881.
27. Steeg PS, Zhou Q. Cyclins and breast cancer. *Breast Cancer Res Treat.* 1998;52(1-3):17-28.
28. Toualbi-Abed K, Daniel F, Guller MC, et al. Jun D cooperates with p65 to activate the proximal kappaB site of the cyclin D1 promoter: role of PI3K/PDK-1. *Carcinogenesis.* 2008;29(3):536-543.
29. Chang H, Qi XY, Claudio J, Zhuang L, Patterson B, Stewart AK. Analysis of PTEN deletions and mutations in multiple myeloma. *Leuk Res.* 2006;30(3):262-265.
30. Adati N, Huang MC, Suzuki T, Suzuki H, Kojima T. High-resolution analysis of aberrant regions in autosomal chromosomes in human leukemia THP-1 cell line. *BMC Res Notes.* 2009;2:153.
31. Kawauchi K, Ogasawara T, Yasuyama M, Otsuka K, Yamada O. The PI3K/AKT pathway as a target in the treatment of hematologic malignancies. *Anticancer Agents Med Chem.* 2009;9(5):550-559.
32. Schmelz K, Sattler N, Wagner M, Lubbert M, Dorken B, Tamm I. Induction of gene expression by 5-Aza-2′-deoxycytidine in acute myeloid leukemia (AML) and myelodysplastic syndrome (MDS) but not epithelial cells by DNA-methylation-dependent and -independent mechanisms. *Leukemia.* 2005;19(1):103-111.
33. Chandras C, Koutmani Y, Kokkotou E, Pothoulakis C, Karalis KP. Activation of phosphatidylinositol 3-kinase/protein kinase B by corticotropin-releasing factor in human monocytes. *Endocrinology.* 2009;150(10):4606-4614.
34. Billottet C, Banerjee L, Vanhaesebroeck B, Khwaja A. Inhibition of class I phosphoinositide 3-kinase activity impairs proliferation and triggers apoptosis in acute promyelocytic leukemia without affecting atra-induced differentiation. *Cancer Res.* 2009;69(3):1027-1036.
35. Silva A, Yunes JA, Cardoso BA, et al. PTEN posttranslational inactivation and hyperactivation of the PI3K/AKT pathway sustain primary T cell leukemia viability. *J Clin Invest.* 2008;118(11):3762-3774.
36. Chiarini F, Fala F, Tazzari PL, et al. Dual inhibition of class IA phosphatidylinositol 3-kinase and mammalian target of rapamycin as a new therapeutic option for T-cell acute lymphoblastic leukemia. *Cancer Res.* 2009;69(8):3520-3528.
37. Steelman LS, Abrams SL, Whelan J, et al. Contributions of the Raf/MEK/ERK, PI3K/PTEN/AKT/mTOR and Jak/STAT pathways to leukemia. *Leukemia.* 2008;22(4):686-707.
38. Min YH, Eom JI, Cheong JW, et al. Constitutive phosphorylation of AKT/PKB protein in acute myeloid leukemia: its significance as a prognostic variable. *Leukemia.* 2003;17(5):995-997.
39. Grandage VL, Gale RE, Linch DC, Khwaja A. PI3-kinase/AKT is constitutively active in primary acute myeloid leukaemia cells and regulates survival and chemoresistance via NF-kappaB, Map-kinase and p53 pathways. *Leukemia.* 2005;19(4):586-594.
40. Hu L, Zaloudek C, Mills GB, Gray J, Jaffe RB. In vivo and in vitro ovarian carcinoma growth inhibition by a phosphatidylinositol 3-kinase inhibitor (LY294002). *Clin Cancer Res.* 2000;6(3):880-886.